Three-Dimensional Organic/Inorganic Hybrid Materials Constructed from One-Dimensional Copper Diamine Coordination Polymers Linked by Bridging Oxoanion Tetrahedra: [Cu(dpe)(MoO_4)] and [Cu(dpe)(SO_4)(H_2O)] (dpe = 1,2-*trans*-(4-pyridyl)ethene)

Douglas Hagrman,[†] Robert C. Haushalter,[‡] and Jon Zubieta*[,†]

Department of Chemistry, Syracuse University, Syracuse, New York 13244, and Symyx Technologies, 420 Oakmead Parkway, Sunnyvale, California 94086

Received July 29, 1997. Revised Manuscript Received September 22, 1997[⊗]

The hydrothermal reaction of $CuSO_4{\cdot}5H_2O$, dpe, MoO_3, and water in the mole ratio 1:2:2:900 at 120 °C for 111 h yielded [Cu(dpe)(MoO_4)] (**1**). Upon omitting the molybdate component, the reaction of $CuSO_4{\cdot}5H_2O$, dpe and water in the mole ratio 1:1:1111 at 120 °C for 72 h yielded [Cu(dpe)(SO_4)(H_2O)] (**2**). The structure of **1** is constructed from $\{Cu(dpe)\}^{2+}$ linear chains bridged through $\{MoO_4\}^{2-}$ tetrahedra into a three-dimensional framework, while that of **2** consists of $\{Cu(dpe)\}^{2+}$ chains bridged through $\{SO_4\}^{2-}$ tetrahedra. However, while the $\{MoO_4\}^{2-}$ units of **1** adopt the η^3-coordination mode, each linking three adjacent chains, the $\{SO_4\}^{2-}$ units of **2** assume η^2-coordination and bridge only two neighboring chains. These differences in $\{EO_4\}^{2-}$ coordination modes are reflected in the dramatically different three-dimensional structures displayed by **1** and **2**. Crystal data: $C_{12}H_{10}CuMoN_2O_4$ (**1**), orthorhombic *Pbcn*, $a = 22.0462(1)$ Å, $b = 12.2957(2)$ Å, $c = 9.7560(2)$ Å, $V = 2644.59(7)$ Å,^{3} $Z = 8$, $D_{calc} = 2.038$ g cm^{-3}; 3202 reflections, $R1 = 0.056$. $C_{12}H_{12}CuN_2O_5S$ (**2**), monoclinic *Pn*, $a = 7.2851(2)$ Å, $b = 9.9062(3)$ Å, $c = 9.1407(2)$ Å, $\beta = 98.207(1)°$, $V = 652.91(3)$ Å, $Z = 2$, $D_{calc} = 1.830$ g cm^{-3}; 1968 reflections, $R1 = 0.027$.

The dramatic expansion in recent years of the crystal "engineering" of organic/inorganic composite materials[1,2] reflects their applications to sorption, photochemistry, electrical conductivity, and catalysis.[3−8] A most successful approach has exploited bifunctional rodlike amine ligands as tethers for the construction of solid phases with diverse and unusual topologies.[9−29] However, the ability to prepare such materials by rational design remains, in general, primitive, as a consequence of the interplay of such factors as ligand donor group geometry, tether length and stereochemistry, solvent, metal coordination preferences and oxidation state, and the identity of the counterion. The structural influences of the anion component are manifest in the structures of [$\{Cu(4,4'\text{-bipy})\}_4Mo_8O_{26}$] and [$\{Cu(4,4'\text{-bipy})\}_4Mo_{15}O_{47}$] in which one-dimensional $\{Cu(4,4'\text{-bipy})\}^{2+}$ coordination polymers are linked through bridging polymolybdate anions and molybdenum oxide one-dimensional chains,

---

[†] Syracuse University.

[‡] Symyx.

[⊗] Abstract published in *Advance ACS Abstracts,* December 1, 1997.

(1) Hoskins, B. F.; Robson, R. *J. Am. Chem. Soc.* **1990**, *112*, 1546.

(2) Bowes, C. L.; Ozin, G. A. *Adv. Mater.* **1996**, *8*, 13.

(3) *Supramolecular Architecture: Synthetic Control in Thin Films and Solids*; Bein, T., Ed.; *ACS Symp. Ser.* **1992**, 499.

(4) *Magnetic Molecular Materials*; Gotteschi, D., Kahn, O., Miller, J. S., Palacio, F., Eds.; *NATO ASI Ser., Ser. E* **1991**, *198*.

(5) *Inorganic Materials*; Bruce, D. W., O'Hare, D., Eds.; Wiley: Chichester, 1992.

(6) *Introduction to Molecular Electronics*; Petty, M., Bryce, M. R., Bloor, D., Eds.; Edward Arnold: London, 1995.

(7) Fujita, M.; Kwon, Y. J.; Sasaki, K.; Yamaguchi, K.; Ogura, K. *J. Am. Chem. Soc.* **1995**, *117*, 7287 and references therein.

(8) Gardner, G. B.; Kiang, Y.-H.; Lu, S.; Asgaonker, A.; Venketaraman, D. *J. Am. Chem. Soc.* **1996**, *118*, 6946.

(9) Blake, A. J.; Champness, N. R.; Chung, S. M.; Li, W.-S.; Schröder, M. *Chem. Commun.* **1997**, 1005.

(10) Blake, A. J.; Hill, S. J.; Hubberstey, P.; Li, W.-S. *J. Chem. Soc., Dalton Trans.* **1997**, 913.

(11) Carlucci, L.; Ciani, G.; Proserpio, D. M.; Sironi, A. *J. Chem. Soc., Dalton Trans.* **1997**, 1801.

(12) Hoskins, B. F.; Robson, R.; Slizys, D. A. *J. Am. Chem. Soc.* **1997**, *119*, 2952.

(13) Losier, P.; Zaworotko, M. J. *Angew. Chem., Int. Ed. Engl.* **1996**, *35*, 2779.

(14) Subramanian, S.; Zaworotko, M. J. *Angew. Chem., Int. Ed. Engl.* **1995**, *34*, 2127.

(15) Batsanov, A. S.; Begley, M. J.; Hubberstey, P.; Stroud, J. *J. Chem. Soc., Dalton Trans.* **1996**, 1947.

(16) Richardson, H. W.; Hatfield, W. E. *J. Am. Chem. Soc.* **1975**, *97*, 835.

(17) Chenggang, C.; Duanjun, X; Yuanzhi, X.; Chaorong, C. *Acta Crystallogr.* **1992**, *C48*, 1231.

(18) Yaghi, O. M.; Guangming, L. *Angew. Chem., Int. Ed. Engl.* **1995**, *34*, 207.

(19) Masciocchi, N.; Cairati, P.; Carlucci, L.; Mezza, G.; Gianfranco, C.; Sironi, A. *J. Chem. Soc., Dalton Trans.* **1996**, 2739.

(20) Kawata, S.; Kitagawa, S.; Kondo, M.; Furuchi, I.; Munakata, M. *Angew. Chem., Int. Ed. Engl.* **1994**, *33*, 1759.

(21) Chen, Z. N.; Fu, D. G.; Yu, K. B.; Tang, W. X. *J. Chem. Soc., Dalton Trans.* **1994**, 1917.

(22) MacGillivray, L. R.; Subramanian, S.; Zaworotko, M. J. *J. Chem. Soc., Chem. Commun.* **1994**, 1325.

(23) Yaghi, O. M.; Li, H. *J. Am. Chem. Soc.* **1995**, *117*, 10401.

(24) Otieno, T.; Rettig, S. J.; Thompson, R. C.; Trotter, J. *Inorg. Chem.* **1993**, *32*, 1607.

(25) Hennigar, T. L.; MacQuarrie, D. C.; Losier, P.; Rogers, R. D.; Zaworotko, M. J. *Angew. Chem., Int. Ed. Engl.* **1997**, *36*, 972.

(26) Robinson, F.; Zaworotko, M. J. *J. Chem. Soc., Chem. Commun.* **1995**, 2413.

(27) Carlucci, J.; Ciani, G.; Proserpio, D. M.; Sironi, A. *J. Chem. Soc., Chem. Commun.* **1996**, 2755.

(28) The influence of flexible spacers has also been addressed. See, for example: Hennigar, T. L.; MacQuarrie, D. C.; Losier, P.; Rogers, R. D.; Zaworotko, M. J. *Angew. Chem., Int. Ed. Engl.* **1997**, *36*, 972.

(29) Wu, L. P.; Yamagiwa, Y.; Kuroda-Sowa, T.; Kamikawa, T.; Munalata, M. *Inorg. Chim. Acta* **1997**, *256*, 158.

S0897-4756(97)00535-8 CCC: $15.00

Table 1. Summary of Crystallographic Data for $[Cu(dpe\}(MoO_4)]$ (1) and $[Cu(dpe)(SO_4)(H_2O)]$ (2)

	1	2
emp formula	$C_{12}H_{10}CuMoN_2O_4$	$C_{12}H_{12}CuN_2O_5S$
formula wt	405.70	359.84
crystal system	orthorhombic	monoclinic
a (Å)	22.0462(1)	7.2851(2)
b (Å)	12.2957(2)	9.9062(3)
c (Å)	9.7560(2)	9.1407(2)
α (deg)	90.0	90.0
β (deg)	90.0	98.207(1)
γ (deg)	90.0	90.0
V (Å^3)	2644.59(7)	652.91(3)
Z	8	2
space group	*Pbcn*	*Pn*
λ (Mo Kα)	0.71073	0.71073
D_{calc} (g cm^{-3})	2.038	1.830
μ, cm^{-1}	25.69	18.56
2θ min, max (deg)	1.85, 28.24	2.06, 28.30
obsd data	3202	1968
no. of parameters	221	198
final $R1$,[a] $wR2$[b]	0.056, 0.082	0.027, 0.073

[a] $R1 = \Sigma||F_o| - |F_c||/\Sigma|F_o|$. [b] $wR2 = [\Sigma(|F_o| - |F_c|)^2/\Sigma w|F_o|^2]^{1/2}$.

Table 2. Atomic Positional Parameters ($\times 10^4$) and Isotropic Temperature Factors (Å^2 $\times$ 10^3) for $[Cu(dpe)(MoO_4)]$ (1)

	x	y	z	U(eq)
Mo(1)	6956(1)	6764(1)	266(1)	12(1)
Cu(1)	7539(1)	9308(1)	−1373(1)	15(1)
O(1)	7106(1)	8100(3)	−278(4)	18(1)
O(2)	7321(2)	5833(3)	−852(4)	27(1)
O(3)	7214(2)	6593(3)	1960(4)	24(1)
O(4)	6177(2)	6534(3)	242(4)	22(1)
N(1)	6763(2)	9719(3)	−2296(5)	18(1)
N(2)	8317(2)	8935(3)	−437(4)	15(1)
C(1)	6557(2)	10722(4)	−2470(6)	19(1)
C(2)	6036(2)	10953(5)	−3225(6)	21(1)
C(3)	5707(2)	10119(4)	−3834(6)	19(1)
C(4)	5921(3)	9066(5)	−3622(8)	36(2)
C(5)	6440(3)	8909(5)	−2868(8)	36(2)
C(6)	8856(2)	8862(4)	−1083(5)	18(1)
C(7)	9401(2)	8792(4)	−370(6)	17(1)
C(8)	9399(2)	8808(4)	1063(5)	13(1)
C(9)	8838(2)	8868(4)	1718(5)	14(1)
C(10)	8316(2)	8929(4)	948(5)	15(1)
C(11)	5172(2)	10354(5)	−4678(6)	24(1)
C(12)	9978(2)	8775(4)	1817(5)	16(1)

Table 3. Atomic Positional Parameters ($\times 10^4$) and Isotropic Temperature Factors (Å^2 $\times$ 10^3) for $[Cu(dpe)(SO_4)(H_2O)]$ (2)

	x	y	z	U(eq)
Cu(1)	9199(1)	9772(1)	4663(1)	10(1)
S(1)	7278(1)	11466(1)	2109(1)	11(1)
O(1)	7079(4)	10538(3)	3362(3)	14(1)
O(2)	6670(4)	10748(3)	684(3)	13(1)
O(3)	9248(4)	11816(3)	2155(3)	17(1)
O(4)	6110(4)	12648(3)	2216(3)	19(1)
O(5)	7642(4)	8466(3)	6145(3)	19(1)
N(1)	9375(5)	8216(3)	3217(4)	14(1)
N(2)	9271(4)	1412(3)	−4001(3)	13(1)
C(1)	9297(6)	6937(4)	3687(4)	19(1)
C(2)	9358(6)	5829(4)	2772(4)	19(1)
C(3)	9553(6)	6017(4)	1284(4)	15(1)
C(4)	9698(6)	7349(4)	807(4)	14(1)
C(5)	9602(5)	8407(4)	1789(4)	14(1)
C(6)	9480(7)	4828(4)	309(5)	18(1)
C(7)	9628(7)	4853(4)	−1123(5)	19(1)
C(8)	9491(6)	3656(4)	−2083(4)	15(1)
C(9)	9037(5)	2367(3)	−1625(4)	13(1)
C(10)	8950(5)	1293(4)	−2583(4)	13(1)
C(11)	9711(6)	2640(4)	−4459(4)	17(1)
C(12)	9841(6)	3772(4)	−3549(4)	19(1)

Table 4. Selected Bond Lengths (Å) and Angles (deg) for $[Cu(dpe)(MoO_4)]$ (1)[a]

Mo(1)−O(4)	1.740(3)	Mo(1)−O(1)	1.758(3)
Mo(1)−O(3)	1.760(4)	Mo(1)−O(2)	1.775(4)
Cu(1)−O(2) #1	1.967(4)	Cu(1)−N(2)	1.996(4)
Cu(1)−N(1)	1.999(4)	Cu(1)−O(3) #2	2.042(4)
Cu(1)−O(1)	2.064(3)	O(2)−Cu(1) #3	1.967(4)
O(3)−Cu(1) #4	2.042(4)	N(1)−C(1)	1.325(7)
O(4)−Mo(1)−O(1)	109.5(2)	O(4)−Mo(1)−O(3)	108.2(2)
O(1)−Mo(1)−O(3)	109.5(2)	O(4)−Mo(1)−O(2)	109.6(2)
O(1)−Mo(1)−O(2)	109.3(2)	O(3)−Mo(1)−O(2)	110.7(2)
O(2) #1−Cu(1)−N(2)	88.1(2)	O(2) #1−Cu(1)−N(1)	90.5(2)
N(2)−Cu(1)−N(1)	178.6(2)	O(2) #1−Cu(1)−O(3) #2	133.0(2)
N(2)−Cu(1)−O(3) #2	90.6(2)	N(1)−Cu(1)−O(3) #2	90.3(2)
O(2) #1−Cu(1)−O(1)	128.7(2)	N(2)−Cu(1)−O(1)	89.8(2)
N(1)−Cu(1)−O(1)	91.1(2)	O(3) #2−Cu(1)−O(1)	98.3(2)
Mo(1)−O(1)−Cu(1)	156.4(2)	Mo(1)−O(2)−Cu(1) #3	147.6(2)
Mo(1)−O(3)−Cu(1) #4	154.0(2)	C(1)−N(1)−C(5)	117.0(4)

[a] Symmetry transformations used to generate equivalent atoms: #1 = $-x + {}^3/_2, y + {}^1/_2, z$; #2 $-x + {}^3/_2, -y + {}^3/_2, z - {}^1/_2$; #3 $-x + {}^3/_2, y - {}^1/_2, z$; #4 $-x + {}^3/_2, -y + {}^3/_2, z + {}^1/_2$; #5 $-x + 1, -y + 2, -z - 1$; #6 $-x + 2, y, -z + {}^1/_2$.

respectively, demonstrating that coordinating anions can impart new dimensions to the design of coordination polymer architectures.[30] As part of our general investigations of the synthesis of oxide phases, we have sought to address the structural roles of the fundamental oxide building blocks, the tetrahedral oxoanions EO_4^{n-} (E = P, S, Mo, and W), in directing the self-assembly of composite materials exploiting copper−diamine coordination polymers as the cation constituent. We report the hydrothermal syntheses and crystal structures of two three-dimensional materials, $[Cu(dpe)(MoO_4)]$ (**1**) and $[Cu(dpe)(SO_4)(H_2O)]$ (**2**) (dpe = 1,2 *trans*-(4-pyridyl)ethene).

Experimental Section

Syntheses were carried out in Parr acid digestion bombs with 23 mL of poly(tetrafluoroethylene) liners or in borosilicate tubes with $^5/_8$ in. outside diameter, $^3/_{32}$ in. wall thickness, and 6 in. length. $CuSO_4{\cdot}5H_2O$, MoO_3, and *trans*-1,2-bis(4-pyridyl)ethylene (bpe) were purchased from Aldrich and used without further purification. Water was distilled above 0.3 MΩ in-housing using a Barnstead Model 525 Biopure distilled water center. Infrared spectra were obtained on a Perkin-Elmer 1600 Series FTIR spectrometer.

Synthesis of $[Cu(dpe)(MoO_4)]$.[1] The reaction of $CuSO_4{\cdot}5H_2O$ (0.052 g), dpe (0.039 g), MoO_3 (0.029 g), and H_2O (10 mL) in the mole ratio 1:1:1:2680 at 120 °C for 44 h yielded light green needles of **1** in 40% yield (based on Mo). IR (KBr pellet, cm^{-1}) 3438 (s, br), 1775 (w), 1708 (w), 1640 (m), 1615 (m), 1429 (m), 1387 (m), 948 (s), 880 (m), 821 (s), 787 (s), 737 (s), 669 (s).

Synthesis of $[Cu(dpe)(H_2O)(SO_4)]$.[2] A mixture of $CuSO_4{\cdot}5H_2O$ (0.050 g), dpe (0.036 g), and H_2O (4 mL, 44% fill volume) in the mole ratio 1:1:1111 was placed in a sealed borosilicate tube and heated at 120° C for 72 h. Blue shards of **2** were isolated in 10% yield based on copper. IR (KBr pellet, cm^{-1}) 3455 (s), 3049 (w), 1505 (w), 1429 (m), 1303 (w), 1176 (s), 1100 (s), 1041 (s), 982 (w), 830 (m), 745 (s), 653 (w), 610 (m), 560 (w), 475 (w).

X-ray Crystallographic Studies. Experimental X-ray data for structures **1** and **2** are displayed in Table 1; atomic coordinates with isotropic temperature factors in Tables 2 and 3; and selected bond lengths and angles are listed in Tables 4 and 5. Structural measurements for compounds **1** and **2** were performed on a Siemens SMART diffractometer with graphite monochromated Mo Kα radiation (λ(Mo Kα) = 0.710 73 Å),

---

(30) Pun intended. See: Hagrman, D.; Zubieta, C.; Rose, R.; Haushalter, R.; Zubieta, J. *Angew. Chem., Int. Ed. Engl.* **1997**, *36*, 873.

Table 5. Selected Bond Lengths (Å) and Angles (deg) for [Cu(dpe)(SO_4)(H_2O)] (2)[a]

Cu(1)−O(1)	1.962(3)	Cu(1)−O(2) #1	1.974(3)
Cu(1)−N(2) #2	2.029(3)	Cu(1)−N(1)	2.047(3)
Cu(1)−O(5)	2.288(3)	S(1)−O(4)	1.459(3)
S(1)−O(3)	1.471(3)	S(1)−O(1)	1.492(3)
S(1)−O(2)	1.495(2)	O(2)−Cu(1) #3	1.974(3)
N(1)−C(1)	1.342(5)	N(1)−C(5)	1.352(5)
N(2)−C(11)	1.340(5)	N(2)−C(10)	1.354(5)
N(2)−Cu(1) #4	2.029(3)	C(1)−C(2)	1.385(5)
O(1)−Cu(1)−O(2) #1	166.67(11)	O(1)−Cu(1)−N(2) #2	90.33(12)
O(2) #1−Cu(1)−N(2) #2	88.91(12)	O(1)−Cu(1)−N(1)	90.93(12)
O(2)− #1−Cu(1)−N(1)	88.37(12)	N(2) #2−Cu(1)−N(1)	173.44(14)
O(1)−Cu(1)−O(5)	99.43(12)	O(2)#1−Cu(1)−O(5)	93.90(11)
N(2) #2−Cu(1)−O(5)	93.94(12)	N(1)−Cu(1)−O(5)	92.20(12)
O(4)−S(1)−O(3)	112.7(2)	O(4)−S(1)−O(1)	108.7(2)
O(3)−S(1)−O(1)	108.9(2)	O(4)−S(1)−O(2)	109.7(2)
O(3)−S(1)−O(2)	107.7(2)	O(1)−S(1)−O(2)	109.1(2)
S(1)−O(1)−Cu(1)	123.3(2)	S(1)−O(2)−Cu(1) #3	132.3(2)
C(1)−N(1)−C(5)	117.3(3)	C(1)−N(1)−Cu(1)	119.7(3)
C(5)−N(1)−Cu(1)	123.1(2)	C(11)−N(2)−C(10)	117.4(3)
C(11)−N(2)−Cu(1) #4	121.7(3)	C(10)−N(2)−Cu(1) #4	120.9(2)

[a] Symmetry transformations used to generate equivalent atoms: #1 = $x + {}^1/_2, -y + 2, z + {}^1/_2$; #2 $x, y + 1, z + 1$; #3 $x - {}^1/_2, -y + 2, z - {}^1/_2$; #4 $x, y - 1, z - 1$.

equipped with a CCD detector. Data were collected at a temperature of 150 K. Data were corrected for absorption using the ψ scan method and corrected for Lorentz and polarization effects. Data processing was accomplished with the SAINT processing program.[31] Direct methods were used to solve all structures using the SHELXTL crystallographic software package.[32] All atoms except hydrogens were refined anisotropically. Neutral atom scattering factors were taken from Cromer and Waber,[33] and anomalous dispersion corrections were taken from those of Creagh and McAuley.[34]

Results and Discussion

Despite a history of applications to synthetic crystal growth,[35] the techniques of hydrothermal syntheses have only recently been exploited in the routine preparation of inorganic materials,[36] most notably in the syntheses of materials of the oxomolybdenum−phosphate[37] and oxovanadium−phosphate and −organophosphonate systems.[38] Hydrothermal reactions, typically carried out at a temperature range of 110−260 °C under autogenous pressure, exploit the self-assembly of the product from soluble precursors. The reduced viscosity of the solvent under these conditions results in enhanced rates of solvent extraction of solids and crystal growth from solution. Since differential solubility problems are minimized, a variety of simple precursors may be introduced, as well as a number of organic and/or inorganic structure-directing (templating) agents from which those of appropriate shape(s) and size(s) may be selected for efficient crystal packing during the crystallization process.[39,40]

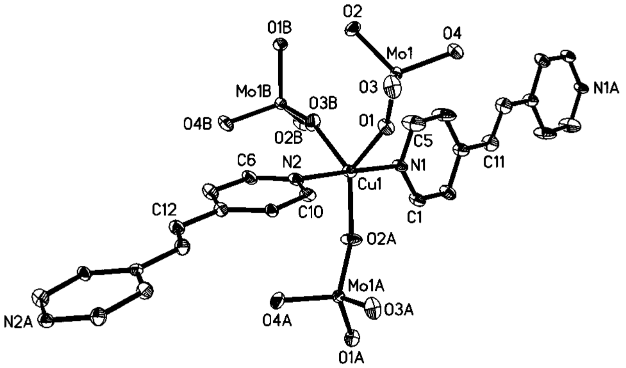

Figure 1. The coordination geometry of the Cu(II) site of [Cu(dpe)MoO_4)] (**1**), showing the atom-labelling scheme and 50% thermal ellipsoids. Selected bond lengths (Å) and angles (°): Cu1−O1, 2.064(3); Cu1−O2a, 1.967(4); Cu1−O3b, 2.042(4); Cu1−N1, 1.999(4); Cu1−N2, 1.996(4); Mo−O, 1.740(3)−1.775(4); N1−Cu1−N2, 178.6(2); O−Cu−O, 98.3(3), 128.7(2), 133.0(2).

Bidentate organodiamine ligands that tolerate reaction temperatures in the range of 110−260 °C and autogenous pressures can be exploited in effecting crystal engineering. New materials may be isolated by varying the length and rigidity of the bidentate ligand, the identity of the metal center, and the anion incorporated into the solid. As part of our ongoing investigations of the applications of hydrothermal synthesis to the preparations of organic/inorganic composite materials, the ligand *trans*-1,2-bis(4-pyridyl)ethene (dpe) was selected as the rigid tether unit linking Cu(II) sites in the polymeric coordination cation $\{Cu(dpe)\}_n^{2n+}$. The anion component may act not only in charge compensating and volume filling roles but also as a ligand to Cu(II) sites. Our previous investigations have suggested that oxoanions are effective ligands for such one-dimensional polymeric chains and may bridge these chains to produce two-dimensional covalent networks and three-dimensional covalent frameworks. The consequences of simple oxoanion substitution are illustrated in the structures of [Cu(dpe)(MoO_4)] (**1**) and [Cu(dpe)(SO_4)(H_2O)] (**2**).

The hydrothermal reaction of $CuSO_4{\cdot}5H_2O$, dpe, MoO_3, and water in mole ratio 1:2:2:900 at 120 °C for 111 h yielded light green cubes of [Cu(dpe)(MoO_4)] (**1**) in 25% yield. The infrared spectrum of **1** exhibited intense bands at 880 and 925 cm^{-1} attributed to ν(Mo═O) and features in the 1300−1600 cm^{-1} range characteristic of dpe. The sulfate phase [Cu(dpe)(SO_4)(H_2O)] (**2**) was prepared similarly as blue shards in the hydrothermal reaction of a mixture of $CuSO_4{\cdot}5H_2O$, dpe, and water in the mole ratio 1:1:1111 at 120 °C for 72 h. The infrared spectrum of **2** exhibited a series of bands at 560, 982, and 1100 cm^{-1}, characteristic of ν(S−O) of the sulfate group, and a series of features in the 1300−1600 cm^{-1} range attributed to dpe.

The structure of **1** is constructed from $\{Cu(dpe)\}^{2+}$ linear chains bridged through $\{MoO_4\}^{2-}$ tetrahedra into a three-dimensional framework. The fundamental struc-

---

(31) SHELXTL, Version 5; Siemens Industrial Automation, Inc., 1994.

(32) Software packages SMART, and SAINT, Siemens Analytical X-ray Instruments Inc., Madison, WI, 1990.

(33) Cromer, D. T.; Waber, J. T. *International Tables for X-ray Crystallography*; Kynoch Press: Birmingham, England, 1974; Vol. IV, Table 2.2A.

(34) Creagh, D. C.; McAuley, J. W. J. *International Tables for X-ray Crystallography*; Kluwer: Boston, MA, 1992; Vol. C., Table 4.2.6.8.

(35) Laudise, R. A. *Chem. Eng. News* **1987**, (*Sept 28*), 30.

(36) Rabenau, A. *Angew. Chem., Int. Ed. Engl.* **1985**, *24*, 1026.

(37) Haushalter, R. C.; Mundi, L. A. *Chem. Mater.* **1982**, *4*, 31 and references therein.

(38) Khan, M. I.; Zubieta, J. *Prog. Inorg. Chem.* **1995**, *43*, 1 and references therein.

(39) Stein, A.; Keller, S. W.; Mallouk, T. G. *Science* **1993**, *259*, 1558.

(40) Gopalakrishnan, J. *Chem. Mater.* **1995**, *7*, 1265.

(41) Zapf, P. J.; Zubieta, J., unpublished results.

(42) Zapf, P. J.; Warren, C. J.; Haushalter, R. C.; Zubieta, J. *Chem. Commun.*, in press.

(43) Hagrman, D.; Zubieta, J., unpublished results.

Table 6. Comparison of General Structural Features for the Members of the Metal′/Organodiamine−Molybdenum Oxide System

compound[a]	structural type	description	M′−Mo−O composition	ref
[Fe(2,2′-bpy)Cl(MoO_4)]	1-D	corner-sharing {MoO_4} tetrhdr and {FeO_3N_2Cl} octhdr	$FeMoO_4$	41
[{Fe(2,2′-bpy)}$_2$(MoO_4)$_3$]	1-D	corner-sharing {MoO_4} tetrhdr and {FeO_4N_2} octhdr	$Fe_2Mo_3O_{12}$	41
[{Fe(2,2′-bpy)}$_2$$Mo_4O_{15}$]	1-D	corner-sharing {MoO_4}, {Mo_2O_7} and {FeO_4N_2} units	$Fe_2Mo_4O_{15}$	41
[Co(2,2′-bpy)Mo_3O_{10}]	2-D	1-D chains of edge-sharing {MoO_6} and {MoO_5} units linked by {CoO_4N_4} octhdr	$CoMo_3O_{10}$	42
[Ni(2,2′-bpy)$_2$$Mo_4O_{13}$]	1-D	β-Mo_8O_{26} clusters linked by {NiO_2N_4} octhdr	$NiMo_4O_{13}$	42
[{Ni(H_2O)$_2$(4,4′-bpy)$_2$}$_2$	3-D	ϵ-Mo_8O_{26} clusters linked by {Ni(H_2O)$_2$(bpy)$_2$}$^{2+}$ chains	$NiMo_4O_{13}$	30
[Cu(2,2′-bpy)Mo_2O_7]	1-D	edge-sharing {MoO_6} octhdr and {MoO_5} tetrhdr linked to {CuO_4N_2} octhdr	$CuMo_2O_7$	42
[{Cu(4,4′-bpy)}$_4$$Mo_{15}O_{47}$]	1-D	edge- and corner-sharing {MoO_6} octhdr	$Cu_4Mo_{15}O_{47}$	30
[{Cu(4,4′-bpy)}$_4$$Mo_8O_{26}$]	2-D	δ-Mo_8O_{26} clusters lined by {Cu(bpy)}$^+$ chains	$Cu_2Mo_4O_{13}$	30
[{Cu(dpe)}$_4$$Mo_8O_{26}$]	2-D	α-Mo_8O_{26} clusters linked by {Cu(dpe)}$^+$ chains	$Cu_2Mo_4O_{13}$	43
[Cu(dpe)MoO_4]	3-D	layers of corner-sharing {MoO_4} tethdr and {CuO_3N_2} tbp linked by dpe	$CuMoO_4$	this work
[Cu(bpa)$_{0.5}$$MoO_4$]	3-D	layers of corner- and edge-sharing {MoO_4} tethdr and {CuO_5N} octhdr linked by bpa	$CuMoO_4$	43

[a] bpy = bipyridine; dpe = 1,2-*trans*-(4-pyridyl)ethene; bpa = bis(4-pyridyl)amine; octhdra = octahedron; tetrhdr = tetrahedron; tbp = trigonal bipyramid.

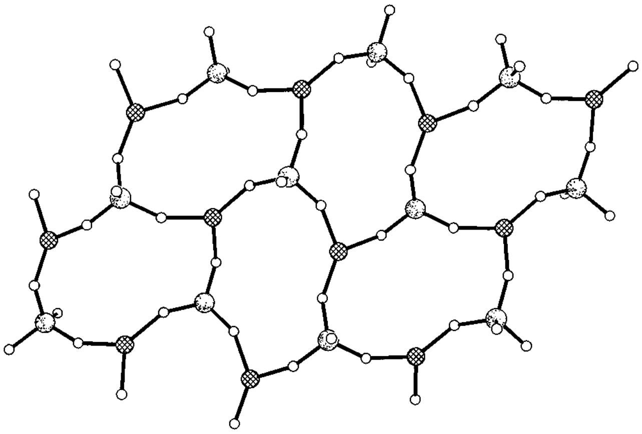

Figure 2. A view parallel to the *b* axis of the {$CuMoO_4$} layer of **1**. Cu sites are cross-hatched; Mo sites are stippled.

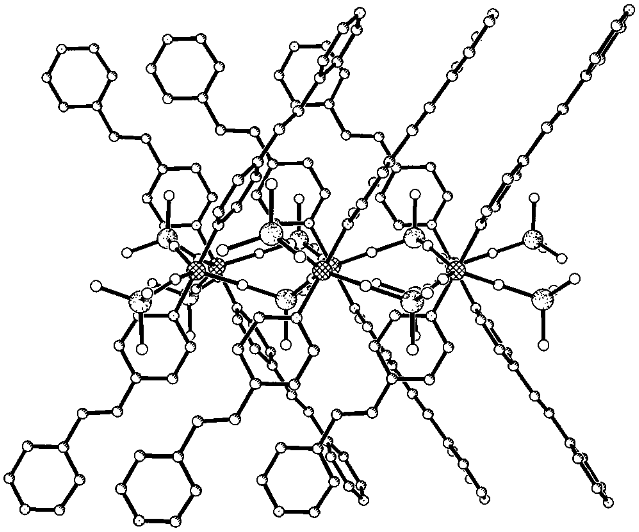

Figure 3. A view of the orientations of the dpe groups relative to the metal oxide plane in **1**.

tural motif, shown in Figure 1, consists of distorted trigonal-bipyramidal Cu(II) centers coordinated to two dpe ligands and three molybdate tetrahedra. The geometry at the Cu sites is defined by three oxygen donors from three {MoO_4}$^{2-}$ groups in the equatorial plane and two dpe nitrogen donors occupying the axial positions. Each molybdate bridges three neighboring Cu sites to produce a bimetallic oxide layer motif {$CuMoO_4$}, illustrated in Figure 2. Each molybdenum site thus possesses one pendent terminal oxo group, which is directed above or below the plane. The connectivity in the plane generates 12-membered {$Cu_3Mo_3O_6$} rings that fuse to propagate the layer structure. The dpe ligands extend from the metal oxide layers at an angle of ca. 35° as shown in Figure 3 and bridge adjacent layers to generate the overall three-dimensional covalent connectivity (Figure 4).

It is noteworthy that a remarkable variety of mixed metal organic/inorganic composites may be prepared from one-dimensional metal-rigid frame organodiamines and molybdenum oxide building blocks. Table 6 summarizes the structural characteristics and compositions of some recently characterized examples. The overall structures adopted in the self-assembly of these materials are dictated not only by reaction parameters of stoichiometry, temperature, pH, concentration, and fill volume but also by the identity and geometry of the organodiamine, the metal component (M′) of the metal−amine polyhedron or linear chain and the geometry and degree of aggregation of the molybdenum oxide anion. Consequently, these materials exhibit a wide range of M′−Mo−O stoichiometries. While such composites are in general thermally stable to 400−500 °C, pyrolysis at higher temperatures results in removal of the organic component. In several cases, monophasic mixed metal oxides are produced. Since the structural characterization and properties of these pyrolysis products are in a nascent stage of development, the potential exploitation of the organic/inorganic composites as precursors to mixed metal oxides remains speculative.

The structural changes engendered by replacing molybdate with sulfate are quite dramatic. As shown in Figure 5, the structural building block is a linear chain of square-pyramidal Cu(II) centers. which are linked through sulfate bridges into a three-dimensional framework. The Cu coordination geometry is defined by trans dpe nitrogen donors and two sulfate oxygen donors in the basal plane with an aquo oxygen in the apical position. In contrast to the η^{3-}{MoO_4}$^{2-}$ groups of **1**, the sulfate units of **2** adopt the η^{2-} modality, bridging two copper sites and projecting two pendent oxo groups

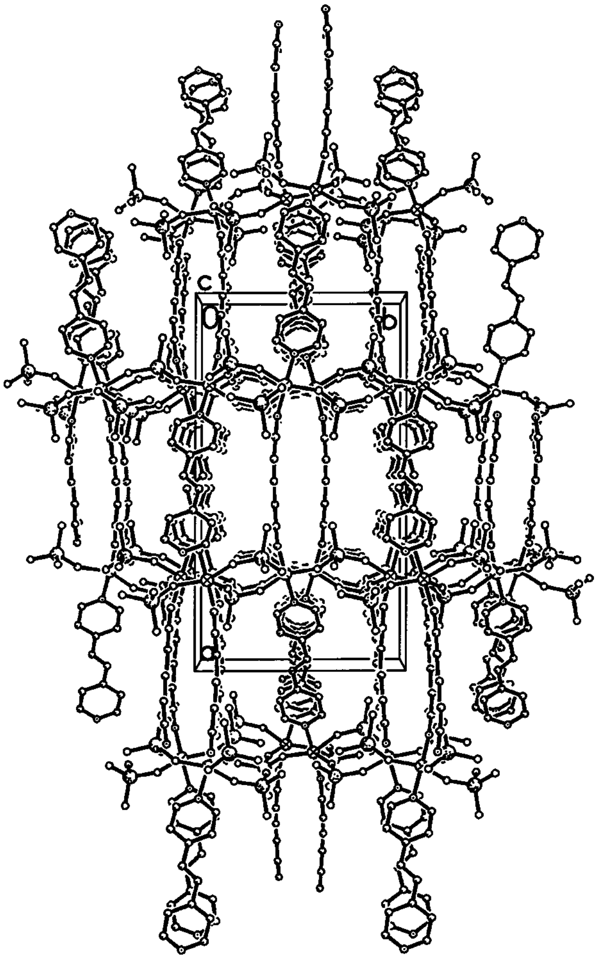

Figure 4. The unit cell contents of **1** viewed parallel to the crystallographic *c* axis.

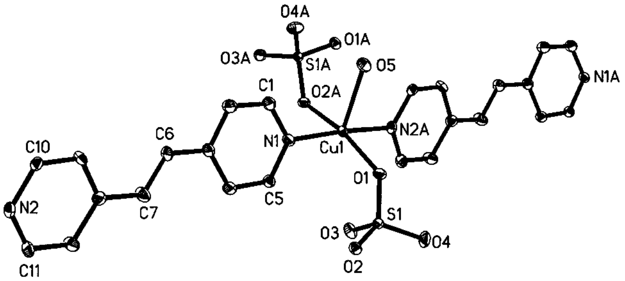

Figure 5. An ORTEP view of the coordination geometry of the Cu(II) site of [Cu(dpe)(SO_4)(H_2O)] (**2**), showing the atom-labelling scheme and the 50% thermal ellipsoids. Selected bond lengths (Å) and angles (°): Cu1–O1, 1.972(3); Cu1–O2a, 1.963(3); Cu1–O5, 2.299(4); Cu1–N1, 2.039(4); Cu1–N2a, 2.036(3); N1–C1–N2a, 174.3(2); O1–Cu1–O2a, 167.3(1); O1–Cu1–O5, 98.8(1); O2a–Cu1–O5, 93.8(1).

into the interchain region. This linkage results in buckled {$CuSO_4$} chains running at approximate right angles to the {Cu(dpe)} chains, producing the weave of linear chains illustrated in Figure 6. The coordination mode of the sulfate restricts the {$CuSO_4$} motif in **2** to chains, in contrast to the layer structure adopted by the {$CuMoO_4$} moiety of **1**.

The incorporation of simple oxoanions into structures constructed from coordination polymers is a recurrent theme of these structural types. In addition to the molybdate phases listed in Table 6, sulfate-containing phases include the title compound **2** and the one- and two-dimensional phases [Cu(H_2O)$_3$(4,4′-bpy)(SO_4)]·$2H_2O$ and [Cu(bpe)$_2$][Cu(bpe)(H_2O)$_2$(SO_4)$_2$], respectively. Nitrate-containing structures include the interpenetrating rating molecular ladder in [Cd{α,α′-xylylbis(4-pyridine)}$_{1.5}$(NO_3)$_2$],[7] the noninterpenetrating ladder structure of [Co(4,4′-bpy)$_{1.5}$(NO_3)$_2$],[13] and the three isomeric structures of [Co{1,2-bis(4-pyridyl)ethane}$_{1.5}$-(NO_3)$_2$].[25]

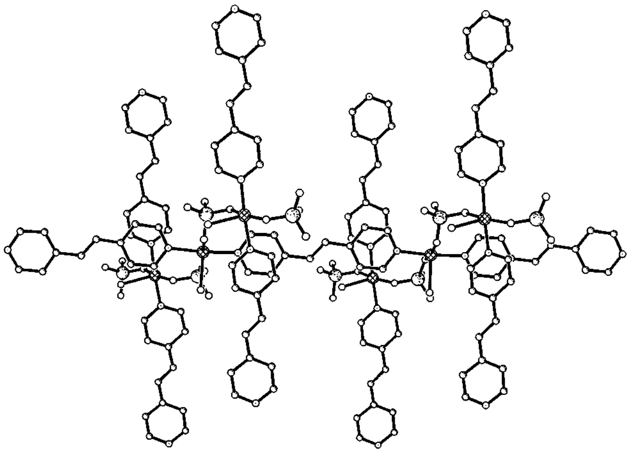

Figure 6. A view of the intersecting {Cu-OS(O_2)O-Cu···} and Cu-$NC_{10}H_{20}N$-Cu···} chains. The Cu centers provide the junction for the chain intersections.

Conclusion

The isolation of the three-dimensional covalent framework materials [Cu(dpe)(MoO_4)] (**1**) and [Cu(dpe)(SO_4)-(H_2O)] (**2**) demonstrates that simple oxoanions may be employed as structural motifs in designing organic/inorganic hybrid materials. Furthermore, coordinating anions influence both the covalent connectivity of the solid and the dimensionality, by directing the self-assembly of such frameworks. Since such anions may adopt various coordination modes, some versatility as constituents of inorganic frameworks is not unexpected.

However, it is also evident that factors such as the ligand tether length and geometry and the identify of the metal component of the coordination polymer cation contribute to the design of the solid-state architecture. The choice of the rigid rodlike diamine ligand introduces variations in catenation length and geometry. Furthermore, the coordination flexibility of the metal center will also contribute to the ultimate framework geometry, as evidenced by the consequences of trigonal-bipyramidal and square-pyramidal geometries at the Cu(II) sites of **1** and **2**, respectively. While the versatility of the fundamental coordination chemistry of the building blocks of these composite solids engenders a diverse structural chemistry, this inherent flexibility complicates attempts at predictable design of such materials.

Acknowledgment. This work was supported by NSF Grant CHE 9617232.

Supporting Information Available: Tables of experimental conditions and crystal data, atomic positional parameters, bond lengths and angles, anisotropic temperature factors, and hydrogen atom positions for **1** and **2** (10 pages); tables of structure factors (13 pages). Ordering information is given on any current masthead page.

CM9705350